Article

Voltage Drop Estimation during Shore Connection with the Use of Motor Drives Modified as Static Frequency Converters [†]

Matouš Vrzala [1,*], Radomír Goňo [1], Břetislav Stacho [2] and Semen Lukianov [2]

1 Department of Electrical Power Engineering, Faculty of Electrical Engineering and Computer Science, VSB-Technical University of Ostrava, 708 00 Ostrava, Czech Republic; radomir.gono@vsb.cz
2 ABB Operation Center Europe (EUOPC), 702 00 Ostrava, Czech Republic
* Correspondence: matous.vrzala@vsb.cz
† This paper is an extended version of our paper published in EPE 2022: 2022 22nd International Scientific Conference on Electric Power Engineering (EPE), Dlouhé Stráně, Czech Republic, 8–10 June 2022; pp. 94–97.

Abstract: Ship-to-shore connection is an important technological element that reduces air pollution in ports. Therefore, ports install facilities that allow mooring ships to connect to the port distribution network. By 2025, this will be mandatory for all ports in Europe. This can be a challenging task in most ports due to the different frequency of the network and ship frequency. This problem can be solved by the use of grid-forming static frequency converters. This solution also brings some other advantages: The ship is not threatened by high shore short-circuit currents, and the port distribution network is not affected by the character of the ship load. However, frequency converter software must include a droop control algorithm to ensure that voltage deviations do not exceed the allowed limits during transients. Typical frequency converters used for shore connection are those developed as static frequency converters (SFCs). However, those converters were not developed for large power outputs, which are needed to power large vessels, such as ferries or cruise ships. This paper proposes motor drives that were modified to operate as SFCs. This approach has quite a lot of advantages which are described in this article. This paper describes both a standard shore connection system without a frequency converter and a solution that includes static frequency converters. The paper then focusses on voltage deviation estimations during connection/disconnection of large load (ferry or cruise ship) to static frequency converters. In this work, a high-voltage shore connection (HVSC) simulation model is developed, including a frequency converter, a shoreside transformer, medium-voltage (MV) connection cables, and a power system of the ship, to analyze in detail the behavior of the system in the case of connection or disconnection of the ship load. The model was made in DIgSILENT PowerFactory for the case of a commercial port in southern France. The model gives credible estimations of voltage drops/surges during transient and steady states.

Keywords: shore connection; voltage drop; grid forming; static frequency converters; DIgSILENT PowerFactory; simulation

1. Introduction

The increasing share of greenhouse gases in the atmosphere and the associated global warming are forcing engineers in all areas to change the technologies used. The maritime industry is no exception, as ships usually burn fuels that emit much more air-polluting gases than conventional diesel used in road transport (in the case of sulfur oxides, the difference is more than a thousand times) [1,2]. This contributes not only to an increase in the share of greenhouse gases in the atmosphere, but also to a deterioration in the air quality of port cities. Auxiliary generators produce carbon dioxide (CO_2), nitrogen oxides (NOx), sulfur oxides (SOx), and particulate matter (PM) [3,4]. For example, in the Turkish port city of Samsun, the analyses resulted in a 12% share of NOx emissions and a 5% share of SO_2 emissions [5]. More than half of these emissions were emitted during the

mooring of ships [5]. This is due to the fact that even when mooring, the ship consumes a significant amount of energy for the operation of pumps, control systems, ventilation, cooling, heating, etc. [6]. Due to the increasingly stringent directives of the International Maritime Organization (IMO) [7] and the EU [8] aimed at reducing the emissions of sulfur oxides, ships are forced to solve these emissions. Shipowners basically have three options to meet their requirements. The first option is to change the fuels they use to power ports in ultra-low-sulfur fuels, such as Marine Gas Oil (MGO). The second option is to invest in scrubber systems that reduce the content of SOx and dust particles. The third option is shore connection. If moored ships are connected to the port city distribution network, emissions can be partially or completely eliminated. The overall rate of emission reductions depends on the energy mix of the area. The European Union has decided that its ports will have to provide the shore connection option by 2025 [9]. However, already from 2005 there has existed a requirement that ships staying at EU ports for more than 2 h are required to use ultralow-sulfur fuel or achieve similar reductions via alternative technologies, including shore connection as an option [9]. The situation in the USA is similar, where, for example, in California ports, the connection to the berth distribution network is already mandatory [9]. In the US, the term "cold ironing" is used as an equivalent to the term shore connection [10].

1.1. Shore Connection Stadardisation

One of the challenges that has prevented faster spread of shore connection technology is the diversity of electricity distribution networks around the world. Incompatibility with the port distribution network has discouraged investors from acquiring this technology. The primary distribution voltage on ships varies from 230 volts to 11 kilovolts [11]. There is also a large variety of loads, and the frequency is sometimes 50 and sometimes 60 Hz [12]. All of this is due to a lack of voltage standardization [2]. The common work of IEC, IEEE, and ISO experts resulted in the development of standards that enable the building of shore connection systems. The HVSC (high-voltage shore connection) standard for vessels with generator power above 1 MVA (IEC/ISO/IEEE 80005-1) was first published in July 2012. The LVSC (low-voltage shore connection) standard for ships under 1 MVA (IEC/ISO/IEEE 80005-3) was first published in August 2014. These two standards enabled the implementation of new shore connection systems, which are consistent with global standards [13]. It is important to mention that, according to the Standards of Training, Certification, and Watch-keeping for Seafarers (STCW) Code, in marine applications, the term high voltage refers to systems above 1 kV [14]. It can be stated that naval HV networks and MV networks on land are synonyms [15]. The second chapter of this paper focuses on shore connection system description according to the above-mentioned standards.

1.2. Frequency Conversion

In the beginning of the development of shore-to-ship power supply, the frequency conversion was provided by a synchronous motor/generator system [16]. Later, the advantage of static frequency converters over rotating motor/generator systems for shore connection was proved [17,18]. These can be installed in the port substation, at the berth, or directly on the ship. A fast dynamic response is one of the most important requirements of frequency converters because it is crucial to prevent a voltage drop caused by large consumers on ship side. The best solution for high-voltage shore connection was then evaluated as a PWM frequency converter with an active front end [19]. It was found that a centralized system with one or more frequency converters placed in a substation is a better solution than distributed topology with one frequency converter placed at each berth [17,19]. Conventional static frequency converters were not developed for large power outputs, which are needed to power large vessels, such as ferries or cruise ships. A new solution is needed, and this solution is described in following paragraphs.

Based on ABB's experience, for a power range between 120 kVA and 5 MVA, it is recommended to use insulated-gate bipolar transistor (IGBT)-based static frequency converters. These frequency converters are low voltage as standard. In combination with

power transformers, they can also be used for ships with high-voltage distribution. Since the 2010s, PCS 100 SFC with a typical rated voltage output of 480 V has been used for shore connection applications. However, PCS 100 SFC could only be used for power outputs of up to 2 MVA. For larger outputs, a medium-voltage, integrated gate-commutated thyristor (IGCT)-based system is recommended. The IGCT represents state-of-the-art in high-power semiconductors and combines both the advantages of a common GTO and the IGBT, i.e., the low conducting losses and very fast transition, respectively. In the 2010s, ABB used PCS 6000, which was able to deliver up to 7 MVA. By parallel operation of PCS 6000 units, the total capacity of frequency converters could be even up to 120 MVA [17,20,21].

However, all frequency converters from the PCS series were developed as static frequency converters, so they were expected to be used in simpler and smaller systems. For complex systems with larger outputs, a new option was found, namely off-grid modification of motor drive. It is a frequency converter developed for driving motors and has modified firmware for use as a static frequency converter. An example of such an ABB low-voltage frequency converter is the ACS880 SFC. This static frequency converter takes advantage of a more robust design that allows outputs of up to 5 MVA (air-cooled), while liquid-cooled units can have outputs up to 6.25 MVA. Moreover, these frequency converters have an accessible DC link to which batteries, supercapacitors, or other sources can be connected. This was not possible with the PCS series. In 2017, ABB presented the medium-voltage frequency converter ACS6080 SFC, which can deliver up to 24 MVA [22,23].

Recent research showed another option—the series connection of three 3.3 kV SiC MOSFETs. It has the potential to replace conventional Si IGBT-based converters for MV applications with improved power density and efficiency [24].

This article is focused on the use of droop-controlled grid-forming low-voltage IGBT frequency converters that are installed in the port substation. The simulation model was created specifically for the ACS880 SFC frequency converter.

Comparative analysis of conventional static frequency converters and the proposed solution was conducted (see Table 1) for power outputs below 1 MVA and over 1 MVA [20,25].

Table 1. Comparative analysis of SFCs.

Parameter	Conventional SFCs	Proposed Solution
price below 1 MVA	lower	higher
price above 1 MVA	higher	lower
size below 1 MVA	smaller	larger
size above 1 MVA	larger	smaller
control	less complex/easier	more complex/more options
maximum power output of single unit	2 MVA	6.25 MVA
maximum power output of parallel units	10 MVA	40 MVA
cooling	only air-cooled	air or liquid-cooled
efficiency	about 95%	about 98%
accessible DC link	no	yes

1.3. Voltage Drop Evaluation

The literature related to droop control and voltage drop calculations during shore connection was studied. There exist only few papers on this topic. According to international standards and high-voltage shore supply quality requirements, the steady-state voltage drop shall not exceed −3.5% of nominal voltage [26]. Important factors that influence voltage drop are power factor, cable length, cable size, and power load. Lower power factor, smaller cable size, larger cable length, and larger power load mean higher voltage drop. According to the measurement in the real port with a 11.4/6.6 kV transformer; 1200 kW load; 0.88 power factor; and cable length of 568 m, the average voltage drop during shore connection was approximately 1.2% [27]. Calculations provided very similar results [27]. Calculations were then made for power loads of up to 8000 kW, cable lengths of up to 2000 m, and a power factor of up to 0.45. The results show that there is a possibility of

overcoming the allowed voltage drop in case of a high power load, a long cable length, and a low power factor [27].

Reference [28] describes shore connection control strategies based on an AC/DC/AC converter. Using rectification control with a double closed loop can effectively rectify the grid and keep the DC side voltage fluctuation small. Different control methods are used on the inverter side at different stages of the grid connection. Pre-synchronization control is applied before closing the circuit breaker to reduce the current surge during shore connection. The V/f control mode is switched to the sag control mode immediately after connection to the grid. After the onboard generator is decommissioned, the control mode is switched back to the V/f control mode. The proposed article shows results for frequency deviations, but no voltage deviation results are available.

The literature about shore connection is lacking articles about dynamic values of voltage drop during transients. Connecting ferries and cruise ships to the port represents a large load for the port. Connecting and disconnecting such a load to the frequency converter in the port can cause significant voltage deviation. Therefore, it is necessary to verify whether this voltage deviation does not exceed the allowed values for a transient or permanent state. The objective of this work is to make a simulation model of the harbor network and simulate three events: connection of the load to the frequency converters; connection of onboard generators with load transfer; and disconnection of the load from frequency converters. All three events are investigated for three types of ships: 11 kV ferry, 6.6 kV cruise ship, and 11 kV cruise ship.

2. Description of Shore Connection System without Frequency Converter

Large cargo and cruise ships (with power input >500 kW) use high voltage for electricity distribution (see Table 2) [11,13]. The production of high-voltage electricity is most often provided by diesel-engine generators or gas-turbine generators. These generators are connected to the main switchboard, from which the compressors, bow thruster, low-voltage transformer, and propulsion transformers are supplied. The low-voltage transformer supplies low-voltage electrical consumers. The propulsion transformers supply the propulsion of the ship. In Figure 1, the single line diagram of the main switchboard is shown, which has a total of 21 cubicles (only half of them are shown).

Table 2. Typical voltage levels for power capacity ranges [11]. (Reproduced in compliance with copyright rules of Global Maritime Energy Efficiency Partnership's website).

Power Capacity	Typical Voltage Levels
<100 kW	230/400/440 V
100–500 kW	400/440/690 V
500–1000 kW	690 V/6.6/11 kV
>1 MW	6.6/11 kV

A total of 20 cubicles serve as feeders for the above-mentioned technologies. An additional cubicle must be added to this switchboard for shore connection (cubicle 21 in Figure 1). This cubicle contains the circuit breaker "B", which is one of the two circuit breakers between the ship's main switchboard and the port.

It is also necessary to install the shore connection switchboard on the ship. It usually has two cubicles (K01 and K02 in Figure 1). The first cubicle (referred to as the incoming cable connection cubicle in Figure 2) contains plugs for connecting cables from the port and an earthing switch. The second cubicle contains the high-voltage circuit breaker "A", the terminals for connecting the cable that further leads to the main switchboard, and the earthing switch of this cable.
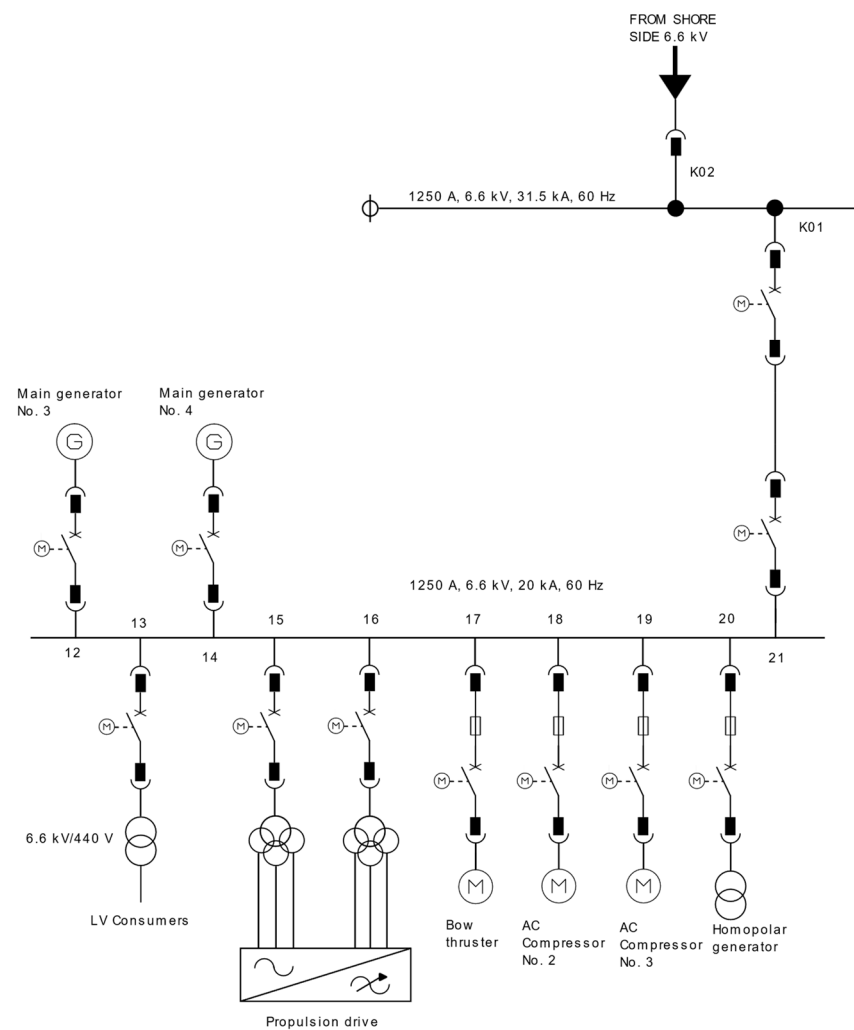
Figure 1. Single line diagram of main switchboard with shore connection.

The main switchboard must also be extended by an automatic synchronizer, which, in cooperation with the automatic voltage regulator, regulates the generator so that it can be phased with the shore distribution network. The automatic voltage regulator must be connected to input signals to obtain information on the mode of the ship and whether the ship network has already been phased to the port distribution network.

The changes also affect the regulators of individual ship propulsions. Before connecting to the port, electricity consumption must be regulated and reduced below a specified level, below which it must be maintained.

The shore connection interface panel (CIP) must be installed for communication with the port. Its main components are cards with digital and analog inputs and outputs. It is necessary to ensure communication between the port and the ship and between the main switchboard in the ship and the shore connection switchboard. The CIP is also used to ensure communication between equipment for regulating the ship's generators and the control system. Two cables with two voltage levels (24 VDC and 110 VDC) lead from the port to the CIP. Some very important signals, such as permission to close (confirmation to the port that the ship is ready to be connected), are sent by signal wires in both cables. Both cables are first connected to the ship in the control socket panel, from which the individual wires are routed to the CIP.
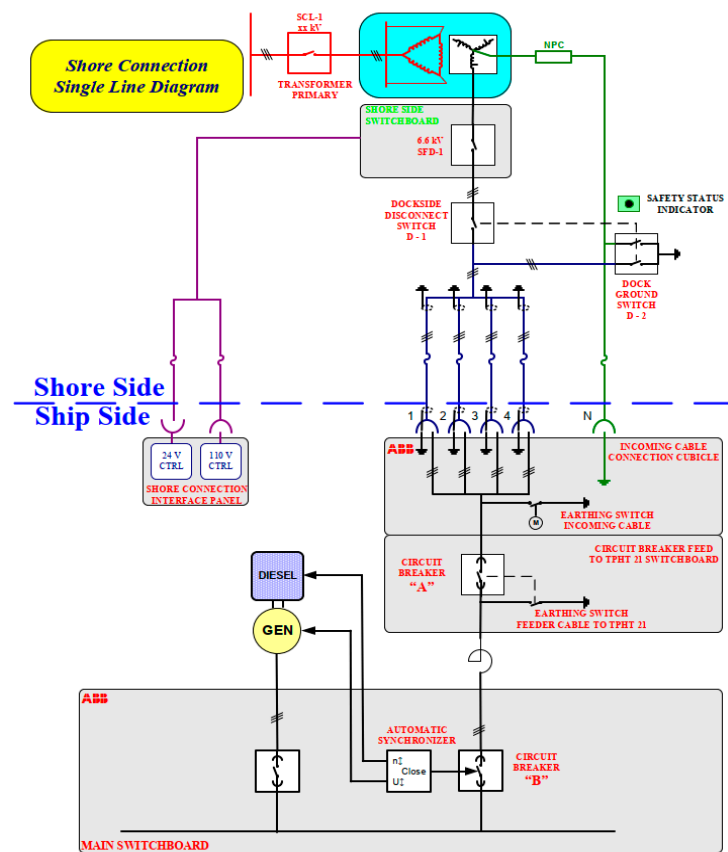
Figure 2. Shore connection single line diagram [29]. (Reproduced with permission from Ronald Jansen, ABB Process Automation Marine & Ports, Houston, TX, USA, 2021).

Another added hardware is the cable tension device. This device measures the tension of the power supply cables to the ship. This is important in the event that the cable or ship starts moving unexpectedly when the ship is electrically connected to the port. The cable tension device operates in three stages. When the tension increases above the first stage level, it sends an alarm to the control system, which is a signal to the operator to go to check the cable. If the tension increases further, then after exceeding the second stage level, the ship generator is switched on with a delay of 10 s. When third-stage tension is exceeded, a command is sent to turn off the circuit breaker, and the ship is electrically disconnected from the port. This minimizes the risk of the supply cables to the ship being unexpectedly turned off, causing the entire ship to lose power.

When a frequency converter is not used, then it is sometimes necessary to limit the short-circuit current that could flow to the main switchboard in the event of a short circuit. The main switchboard can be designed for short-circuit currents lower than the transformer in the port. At the top of the single line diagram in Figure 1, it can be seen that the busbar in the shore connection switchboard is rated for a short-circuit current of 31.5 kA, while the busbar of the main switchboard is rated for 20 kA. For these reasons, it is necessary to install a reactor between these two cabinets that limits the short-circuit current, as can be seen in Figure 2. When using a frequency converter, the problem is the opposite, and it must be ensured that the frequency converter will provide enough short-circuit current for the proper function of protection devices. It can be quite a challenging task because some semiconductor technology does not allow overcurrent capability. The solution is either to oversize a converter or to operate more converters in parallel.

3. Description of Shore Connection System with Frequency Converter

Shore connection can be a challenging task in most European ports due to the different frequency of the network and the frequency of the ship. Frequency on ships is usually

60 Hz, but the frequency of distribution networks in Europe and many other countries in the world is 50 Hz. This problem can be solved by an installation of static frequency converters. These converters must be developed for forming a grid, not for controlling motors. For that reason, their hardware and software differ from motor drives. The system functions by converting input AC power through a rectifier to a DC link and then through an inverter to produce a clean, full sine-wave output at the new frequency and voltage. The SFC system is constructed using power electronic modules (IGBT). An example of such a system is ABB PCS100 SFC, which can be seen in Figure 3. An isolation transformer is required at either the input or output of the PCS100 SFC for correct operation. These SFCs are constructed using pairs of rectifier and inverter power modules (module pairs).
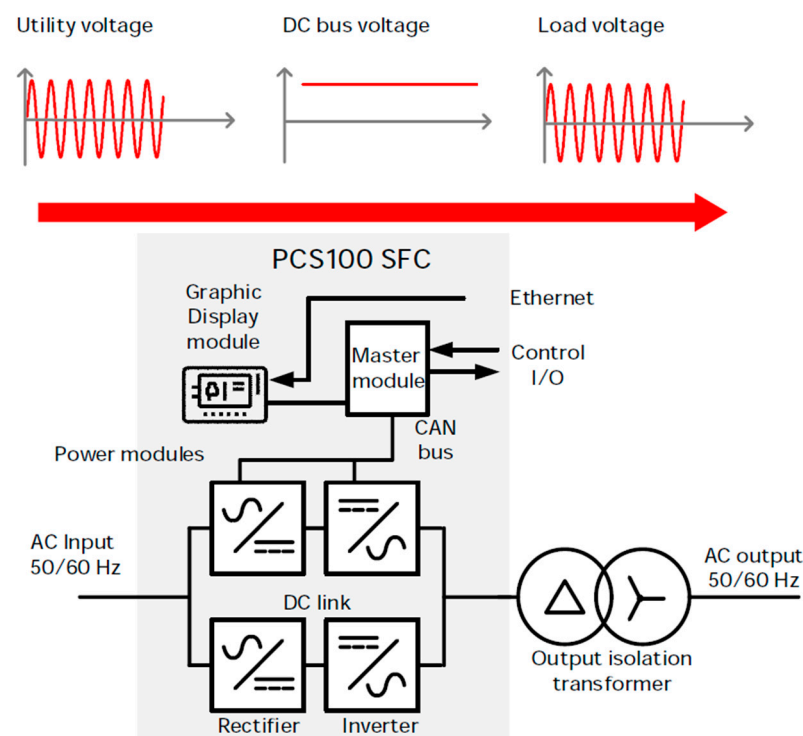
Figure 3. An example of static frequency converter system used for shore connection [20]. (Reproduced with permission from ABB Process Automation Marine & Ports, 2021).

However, these SFCs were developed for smaller systems, and, for example, one PCS100 unit has a maximum power output of only 2 MVA. In parallel operation of more units, this output can be up to 10 MVA. In the case of medium-voltage static frequency converters with IGCT technology, maximum power output can be higher as was described in the first section of this article. To enable shore connection of large vessels, static frequency converters with even higher outputs are needed. For that reason, a new option was investigated: off-grid modification of motor multidrive. Multidrive is a system with one IGBT rectifier called ISU (IGBT supply unit), which rectifies three-phase AC currents for the intermediate DC link that supplies IGBT inverter units that run the motor. The system is shown in Figure 4. The advantage of this system is that only one rectifier unit is needed for more inverter units. An essential part of the IGBT supply unit is the LCL filter, which suppresses AC voltage distortion and current harmonics.

No.	Description
1	AC supply
2	Input (AC) fuses
3	Supply unit
4	DC bus
5	Inverter DC fuses (with or without a DC switch-disconnector)
6	Inverter units (in this example, one of the two units consists of two inverter modules connected in parallel)
7	Brake unit (brake resistors not shown)
8	Motor(s)
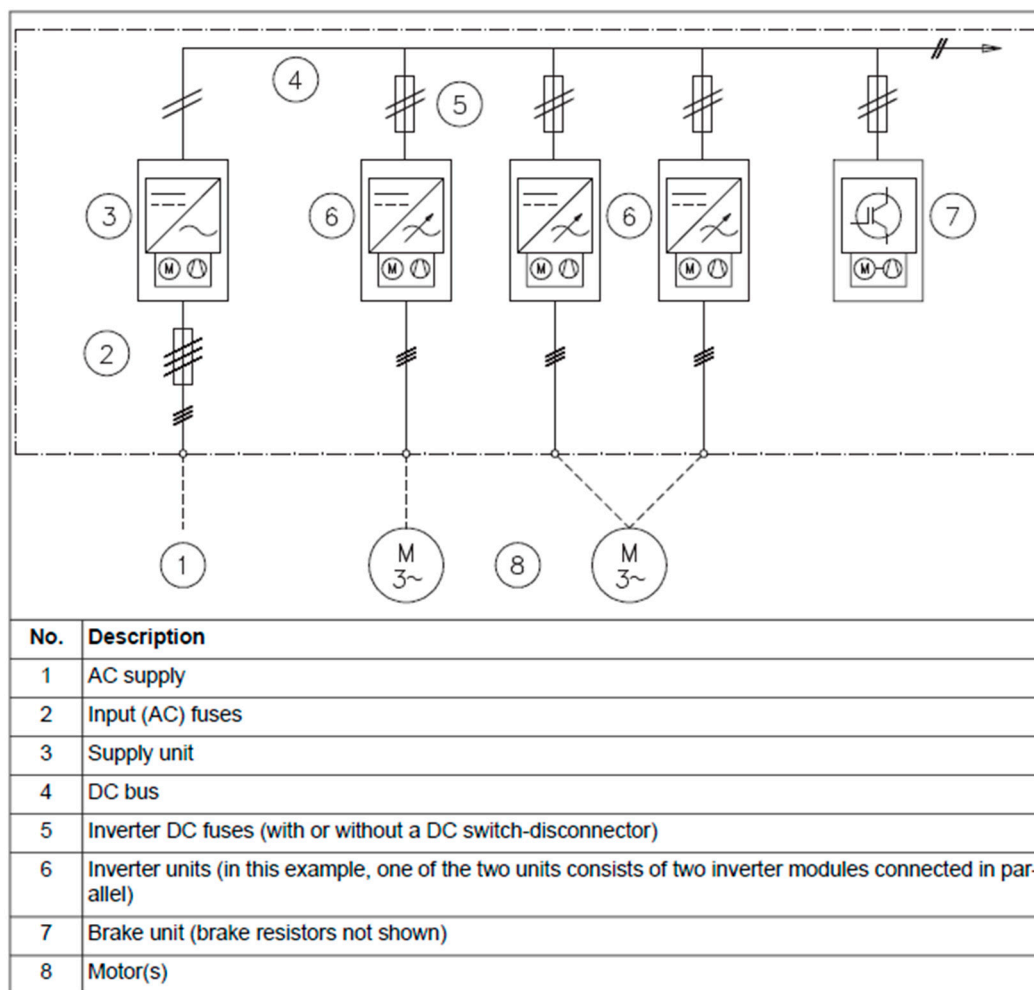
Figure 4. Multidrive system topology [25]. (Reproduced with permission from ABB Process Automation Marine & Ports, 2020).

It was investigated if these robust systems can be applicable for a very different use–shore connection. It was found that this same hardware can be updated with new firmware called OGC (optimal grid control) to be used as static frequency converters. The system is then similar: 50 Hz AC distribution network of the port is rectified by the IGBT supply unit, which supplies a DC link. The advantage of an accessible DC link in port is that it allows the installation of additional DC/DC converters on the DC bus to allow an external source (such as batteries, photovoltaics, and supercapacitors) power supply to be connected. The number of IGBT inverter units can be connected to a DC link and used to supply a 60 Hz AC distribution network of the ship. The whole system is shown in Figure 5. An example of such an ABB low-voltage frequency converter is the ACS880 SFC. This static frequency converter takes advantage of a more robust design that allows outputs of up to 5 MVA (air-cooled); liquid-cooled units can have outputs of up to 6.25 MVA.
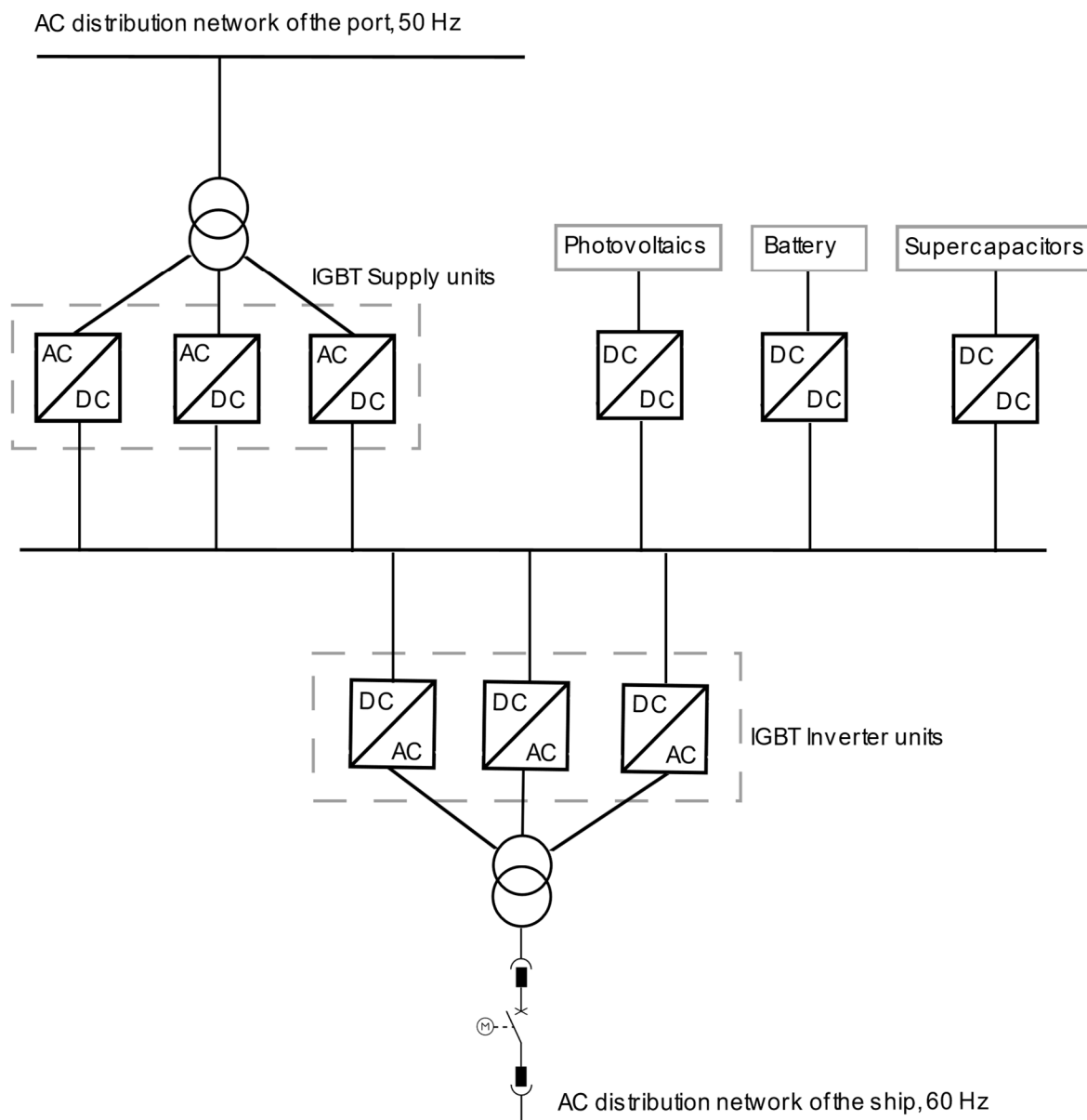
Figure 5. Multidrive system used as static frequency converter system.

4. Materials and Methods

Power system study calculations were computed by means of digital planning software DigSILENT Power Factory 2021 SP 2, which is a power system analysis software for applications in generation, transmission, distribution, and industrial systems.

According to [27], the resulting voltage drop can be calculated by the sum of voltage drops on individual components.

For power cables, the voltage drop can be calculated approximately with the following formula [30]:

$$V_{\text{Drop,Cable}} = \sqrt{3}(IR\cos\varphi \pm IX\sin\varphi) \tag{1}$$

where $V_{\text{Drop,Cable}}$ is the voltage drop for power cables; I is the current of loads on ships when berthing (A); φ is the angle of power factor for the load; R and X are the resistance (Ω) and reactance (Ω) of the power cables. For inductive load (most cases), "+" is used, and for capacitive load, "−" is used.

For the power transformer, the voltage drop can be calculated approximately with the following formula [30]:

$$V_{\text{Drop,Tr}} = V_{\text{Tr2}} \cdot (R_\% \cos \varphi \pm X_\% \sin \varphi) \cdot \frac{S_{\text{Load}}}{S_{\text{n}}}, \tag{2}$$

where $V_{\text{Drop,Tr}}$ is the voltage drop for power transformers; V_{Tr2} is the rated voltage of secondary terminal of the transformer; $R_\%$ and $X_\%$ are the percent resistance (%) and reactance (%) of the transformer, respectively; S_{Load} is the loading (kVA) of the transformer; and S_{n} is the rated power (kVA) of the transformer.

The resulting voltage drop gives us useful information about adjusting the tap-changer position.

However, for the calculation of actual values of voltage drop during droop control, a more complex approach is needed. The converter was modelled using the Static Generator model from the DIgSILENT PowerFactory library, which matches the ABB ACS880-207 frequency converter. The control chain of the frequency converter is based on the droop-controlled grid-forming converter model, which is defined in the DigSILENT Global library. The apparent output power of the ACS880-207-3080A-7 ISU is assumed to be limited by 2700 kVA. The converter operates in optimal grid control mode. Active and reactive power of the supplied grid are controlled by means of 1% P/f and Q/U droop.

Voltage regulation is implemented on the basis of the principle that reactive power contribution depends on the deviation in system voltage from the desired reference voltage value. This can be described mathematically by the following equation:

$$\Delta V = V_{\text{ref}} - q \cdot m_q - v_{meas}, \tag{3}$$

where ΔV is the voltage error; V_{ref} is the reference voltage; q is the measured reactive power; m_q is the droop gain; and v_{meas} is the measured terminal voltage.

Frequency regulation is implemented on the basis of the principle that the difference between generated active power and load causes a deviation in the system frequency from the desired reference frequency. This can be described mathematically by the following equation:

$$(f_{\text{ref}} - f_{meas})m_{\text{p}} + (p_{set} - p_{\text{reg}}) = 0, \ m_{\text{p}} = \frac{1}{\rho}, \tag{4}$$

where f_{ref} is the reference frequency; f_{meas} is the measured frequency; ρ is the droop coefficient; m_{p} is the effective gain; p_{set} is the operating power set-point; and p_{reg} is the active power reference. If the system frequency deviates from the reference frequency, p_{reg} will change accordingly. In steady-state conditions, p_{reg} will be equal to p_{set}.

The used control diagram of the grid-forming converter is shown in Figure 6. This diagram consists of individual blocks. There are three user inputs to these blocks: p_set, q_set, and u_ref. There are also two measurement blocks, which means that voltage and current must be measured. The power calculation block uses measured voltage and current for active and reactive power calculation, which are sent to the droop control block. The droop control block also receives information about the measured frequency from the voltage measurement block and the desired value of voltage from the voltage control block. The output voltage calculation block uses outputs from the droop control block and, in addition, outputs from the virtual impedance block. Virtual impedance is a way to alter the control of an inverter so that it appears as though an additional impedance is inserted between the inverter and the load in the physical circuit. This makes it possible to change the effective impedance between the inverter and the load. Finally, the output of the output voltage calculation block is connected to the converter.

The function of the droop control block is shown in detail in Figure 7. This diagram explains the calculation procedure of droop control loop.
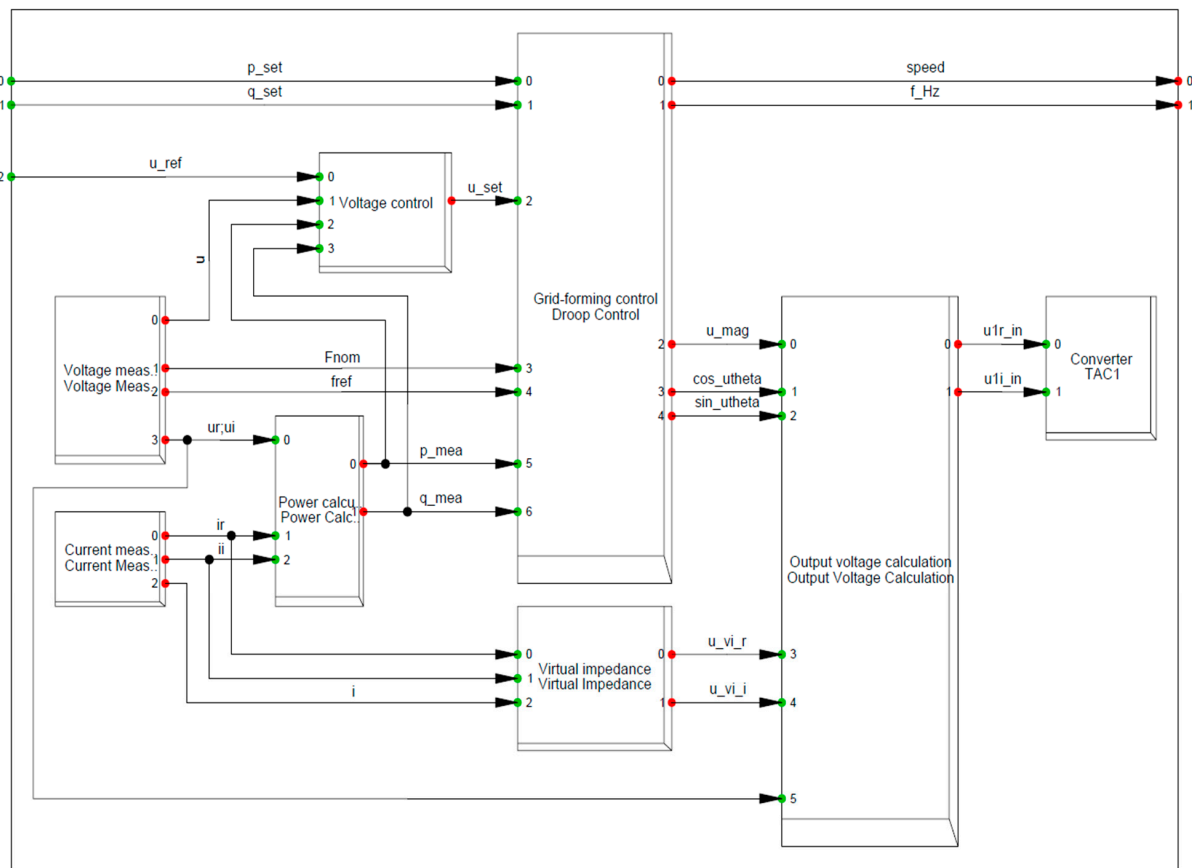
Figure 6. Control diagram of grid-forming converter.
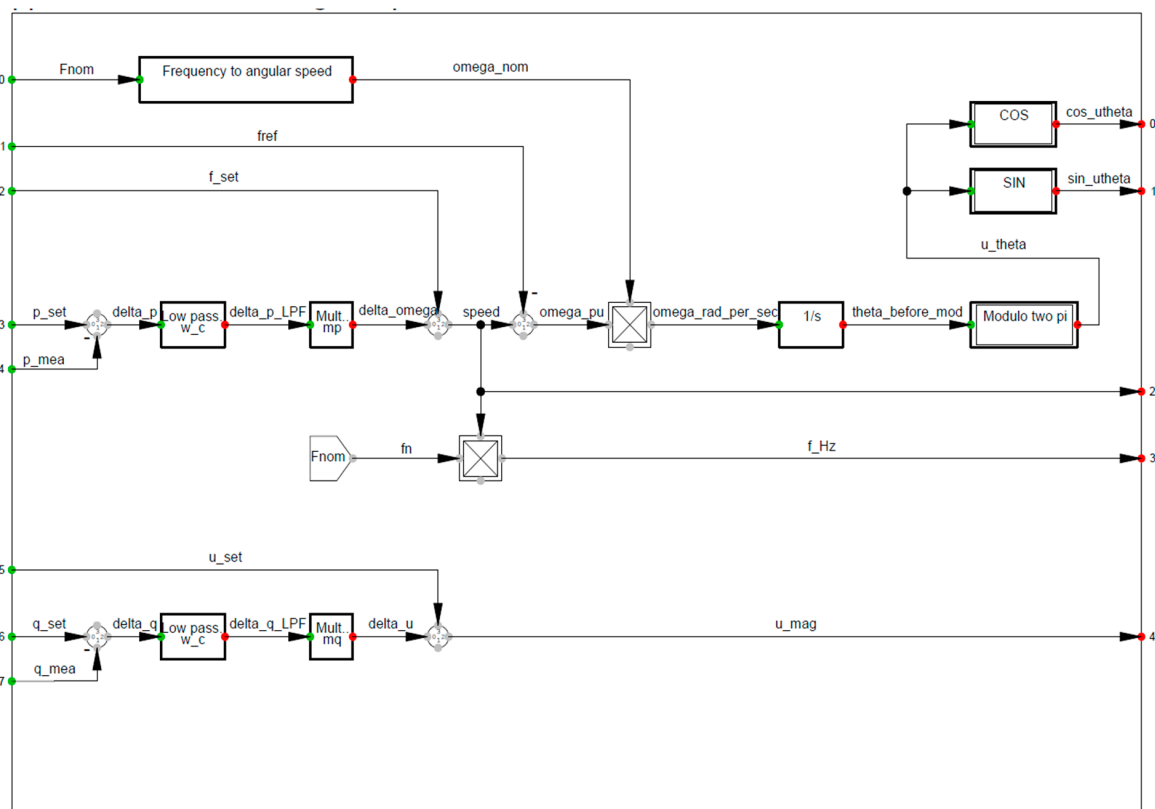
Figure 7. Grid-forming droop control diagram.

Based on the single line diagram of the distribution network of the port and the nominal values of the equipment, the network model was created using DigSILENT Power Factory 2021 SP-2 software (see Appendix A). The network model contains the part from frequency converters to ship. This part consists of four identical frequency converters, converter busbars, three two-winding and two three-winding power transformers, cables between power transformer and quay, quay busbars, and two types of ship generators.

The transformer parameters are shown in Table 3.

Table 3. Parameters of used transformers.

Parameter	Two-Winding Transf.	Three-Winding Transf.
Rated power, kVA	2800	6000
Rated frequency, Hz	50	60
Rated voltages, kV/kV	11/0.66	12 (6.928)/0.66/0.66
Vector group	Ynd11	Yd11d11 (Dd0d0)
Impedance, %	6	6
Zero sequence impedance, %	5.52	5.52
Load losses, kW	20.385	50
No-load losses, kW	3.081	10
No-load current, %	0.13	0.1
Tap changer	Off-load, $\pm 2 \times 2.5\%$	Off-load, $\pm 2 \times 2.5\%$

The parameters of the ship generators are shown in Table 4.

Table 4. Parameters of used generators.

Parameter	Ferry Generator	Cruise Ship Generator
Nominal apparent power, kVA	2700	11,500
Nominal voltage, kV	10.5	10.5 (6.6)
Power factor	0.8	0.8
Stator resistance, p.u.	0.0504	0.0504
Stator leakage reactance, p.u.	0.1	0.1
Synchronous reactance xd, p.u.	1.5	1.5
Synchronous reactance xq, p.u.	0.75	0.75
Transient time constant Td', s	0.53	0.53
Transient reactance xd', p.u.	0.256	0.256
Subtransient time constant Td'', p.u.	0.03	0.03
Subtransient time constant Tq'', p.u.	0.03	0.03
Subtransient reactance xd'', p.u.	0.168	0.168
Subtransient reactance xq'', p.u.	0.184	0.184
Acceleration time constant, s	5	5

5. Results and Discussion

Simulation was carried out using DigSILENT Power Factory 2021 SP 2. The simulation step size in the range of 0.2 to 0.5 ms was used, which is enough for the calculation of electromechanical transients. Used simulation parameters are shown in Table 5.

Table 5. Parameters for simulation.

Parameter	Value
Converter apparent power, MVA	2.7
Converter active power, MW	2.16
Converter reactive power, MVAr	1.62
Converter power factor	0.8
Active power droop coefficient, p.u.	0.01
Reactive power droop coefficient, p.u.	0.05
Low-pass filter cut-off frequency, rad/s	60
Time constant for low-pass filter, s	0.0001

Table 5. *Cont.*

Parameter	Value
Basic virtual resistance, p.u.	0.006
Basic virtual reactance, p.u.	0.006
Proportional factor for additional resistance, p.u.	8
Proportional factor for additional reactance, p.u.	8

First, a steady-state voltage drop was calculated to define the tap-changer position of the secondary windings of transformers. The voltage drop during transient events was then calculated.

The voltage drop was calculated for three events:

1. Connection of the load to the frequency converters
2. Connection of onboard generators with load transfer
3. Disconnection of the load from frequency converters.

For every event, voltage drop was calculated for three types of ship:

- 11 kV ferry mode (2700 kVA, $\cos\varphi = 0.8$)
- 11 kV cruise mode (11,500 kVA, $\cos\varphi = 0.8$)
- 6.6 kV cruise mode (11,500 kVA, $\cos\varphi = 0.8$).

The results for off-load tap-changer positions are as follows:

- +5% for 11 kV ferry mode (2700 kVA)
- +3.6% for 6.6 kV cruise mode (11,500 kVA)
- +5% for 11 kV cruise mode (11,500 kVA).

During the simulation of 2700 kVA ferry operation, the most left branch (1A) of the shore network was active as can be seen in Figure A1. Only one frequency converter was active. During the simulation of 11,500 kVA cruise operation, all four frequency converters and both three-winding transformers were active. Quai 2B-BD2B3 was used because it has the longest cable and therefore the worst results from all three cruise quays.

The voltage drop during transient events was calculated for both the low-voltage (top part of figures) and high-voltage (bottom part of the figures) part of the network. Maximum voltage drop/surge values are shown in Table 6. LVBB refers to low-voltage busbar. QUAI_1A refers to high-voltage busbar in the ferry quay. QUAI_2B-BD2B3 refers to high-voltage busbar in the cruise quay.

a. *Connection of the load to the frequency converters*

Table 6. Results of maximum voltage drop/surge values during transient events.

Event	11 kV Ferry Mode		11 kV Cruise Mode		6.6 kV Cruise Mode	
Side:	LV	HV	LV	HV	LV	HV
Connection of the load, %	4.93	5.21	4.46	5.59	4.57	4.6
Connection of onboard generators, %	8.45	8.43	8.72	8.02	9.55	8.29
Disconnection of the load, %	5.22	10.49	4.79	8.61	4.79	10

Initially, when the onboard CB is open, there are no loads connected to the converter station. The frequency converter is operated at a 1 p.u. voltage level. The voltage level at ship connection terminals is equal to 1.05 p.u. in ferry operation mode and in cruise operation mode with 6.6 kV topology. In cruise operation mode with 11 kV topology, the voltage level at ship connection terminals equals to 1.036 p.u. After a period of 2 s, the onboard CB is closed, and the load is connected. When the load is connected to the conversion station, the voltage drops, and the droop control starts acting until a new steady state is reached. According to the simulation results, the new steady state is reached in 70–80 ms.

i.   Connection of the load to frequency converters in 11 kV ferry mode

After the connection of the load voltage to the ship connection terminals, it drops to approximately 0.948 p.u. (see Figure 8). When a transient process is finished, the voltage level during a new operation mode is established on a level equal to 1 p.u. at ship connection terminals. There is no exceeding of voltage limits observed.
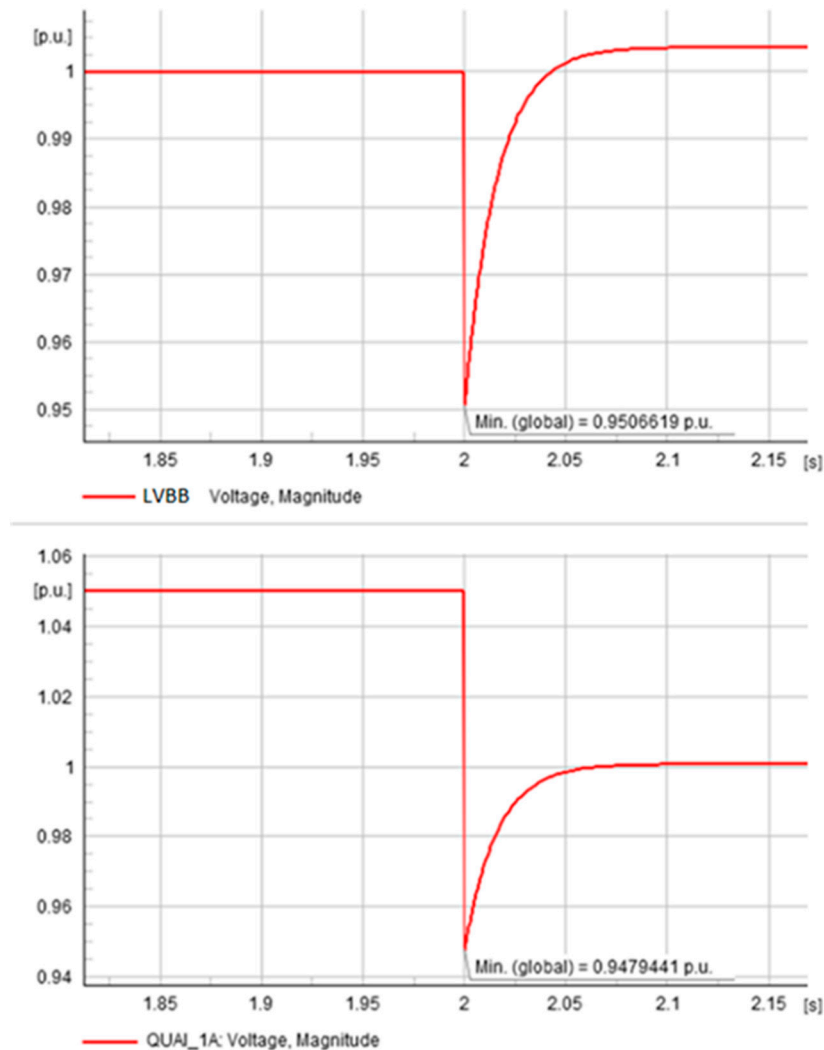
Figure 8. Terminal voltages during connection of the load in 11 kV ferry operation mode.

ii. Connection of the load to frequency converter in 11 kV cruise operation mode

After connection of the load voltage at ship connection terminals, it drops to approximately 0.944 p.u. (see Figure 9). When a transient process is finished, the voltage level during a new operation mode is established on a level equal to 1 p.u. at ship connection terminals. There is no exceeding of voltage limits observed.

iii. Connection of the load to frequency converter in 6.6 kV cruise operation mode

After the connection of the load voltage to the ship connection terminals, it drops to approximately 0.954 p.u. (see Figure 10). When a transient process is finished, the voltage level during a new operation mode is established on a level equal to 1 p.u. at ship connection terminals. There is no exceeding of voltage limits observed.
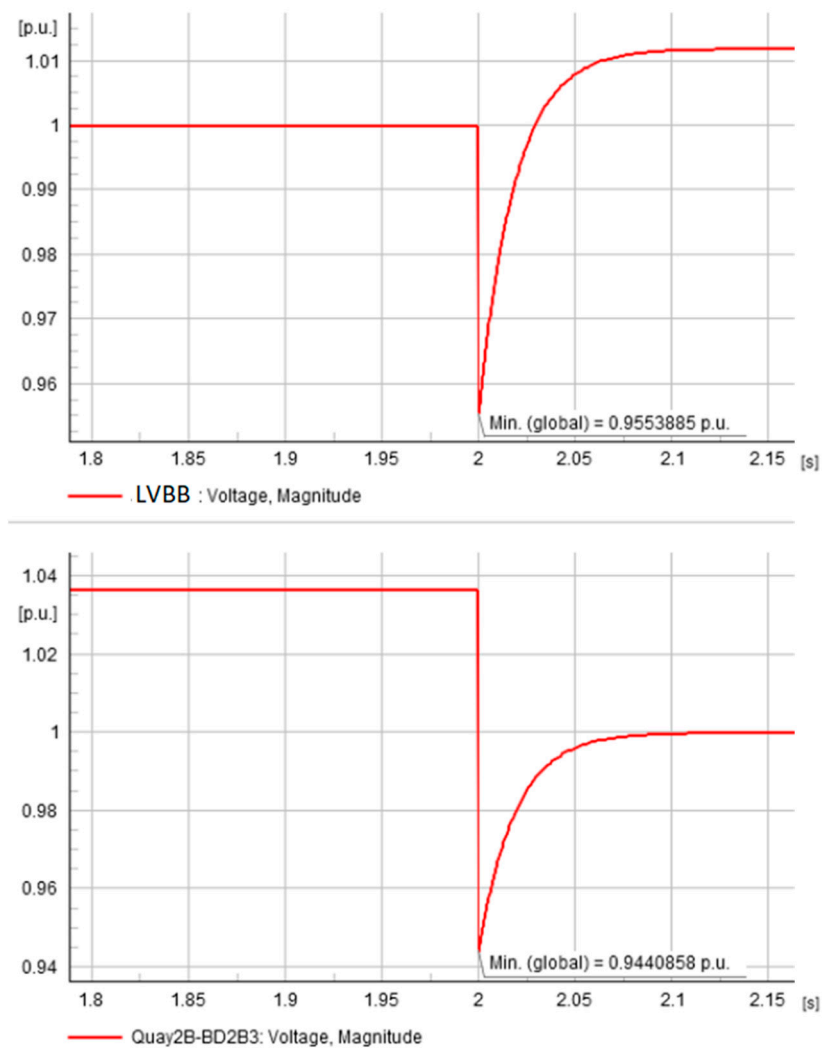
Figure 9. Terminal voltages during connection of the load in 11 kV cruise operation mode.

b. *Connection of onboard generators with load transfer*

In this chapter, simulation results of voltage deviations for load transfer events are provided.

Initially, when the onboard CB is open, the network consists of two isolated grids: from the frequency converter to the onboard CB and from the onboard CB to the vessel generators. It is assumed that the converter and generator are both operated on the same frequency and with the same voltage angle at the point of ship connection. At the same time, the operating voltage of the synchronous generator is 1 p.u., and hence, the voltage difference between the ship connection terminal and the operational voltage of the synchronous generator could exist, but according to simulation results, this voltage difference does not exceed 0.05 p.u.

In a period of 2 s, when the CB is closing, synchronization of the vessel generator with the frequency converter begins. Synchronization is usually followed by a voltage drop and synchronizing currents. For the simulations provided in this chapter, the closing of the CB is accompanied by a load transfer from the onboard generators to the frequency converters, which, in turn, makes the voltage drop even higher. The load transfer is characterized by step change of the power dispatched from the synchronous generator, which results in worst case results in terms of voltage drop.

After closing the onboard CB and after the load transfer from generators to converters, AVR (automatic voltage regulator) and PSS (power system stabilizers, if present) of generators start acting concurrently with droop control of the frequency converter to restore

the voltage level and operated frequency of the network until the time when a new steady state is reached.
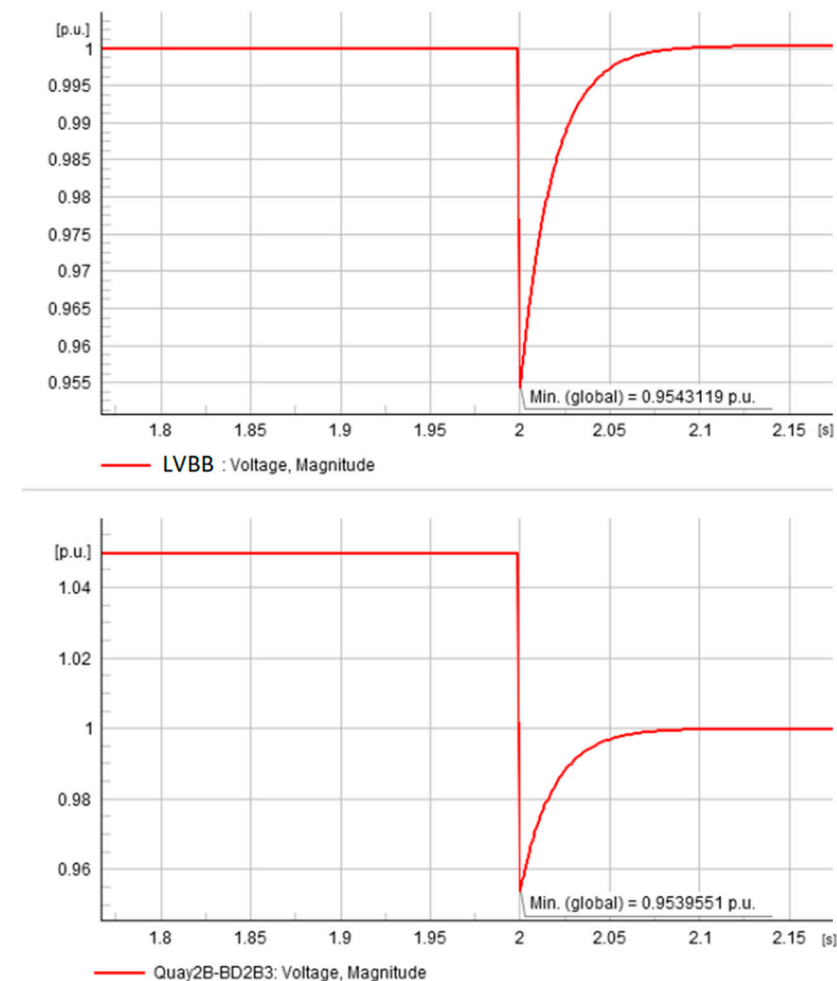
Figure 10. Terminal voltages during connection of the load in 6.6 kV cruise operation mode.

i. Connection of onboard generators with load transfer in 11 kV ferry operation mode

In this chapter, voltage deviations at ferry berths during transfer of 540 kW power are investigated. After closing the onboard CB and after load transfer event, the voltage at the ship connection terminals drops to approximately 0.915 p.u. (see Figure 11). When a transient process is finished, the voltage level during a new operation mode is established at a level equal to 1 p.u. at the ship connection terminals. There is no exceeding of voltage limits observed.

ii. Connection of onboard generators with load transfer in 11 kV cruise operation mode

In this chapter, voltage deviations at cruise berth during transfer of 2300 kW power are investigated.

After connection of the load voltage at the ship connection terminals, it drops to approximately 0.919 p.u. (see Figure 12). When a transient process is finished, the voltage level during a new operation mode is established at a level equal to 1 p.u. at ship connection terminals. There is no exceeding of voltage limits observed.

iii. Connection of onboard generators with load transfer in 6.6 kV cruise operation mode

In this chapter, voltage deviations at cruise berth during transfer of 2300 kW power are investigated. The conversion station is run under very similar initial conditions as in previous section. The difference is in the power supply conditions and in tap position of power transformers.
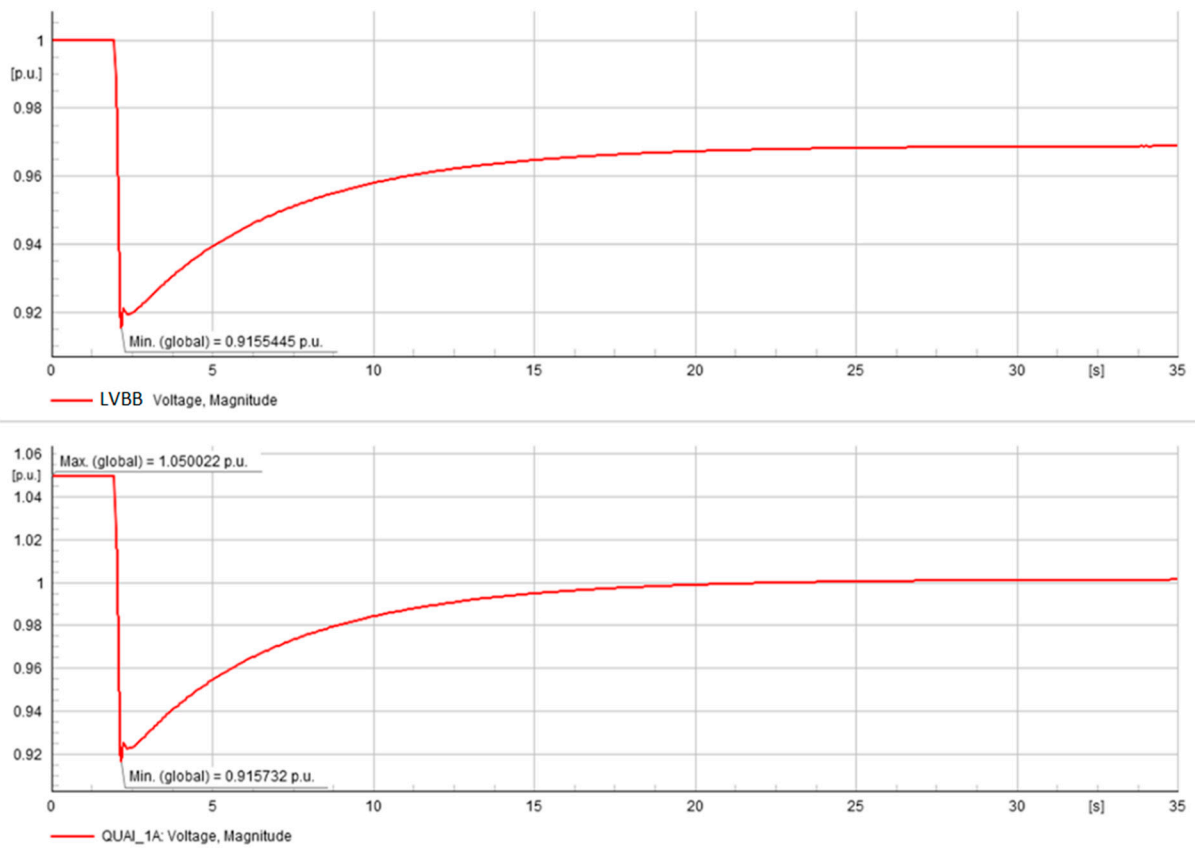
Figure 11. Terminal voltages during load transfer in 11 kV ferry operation mode.
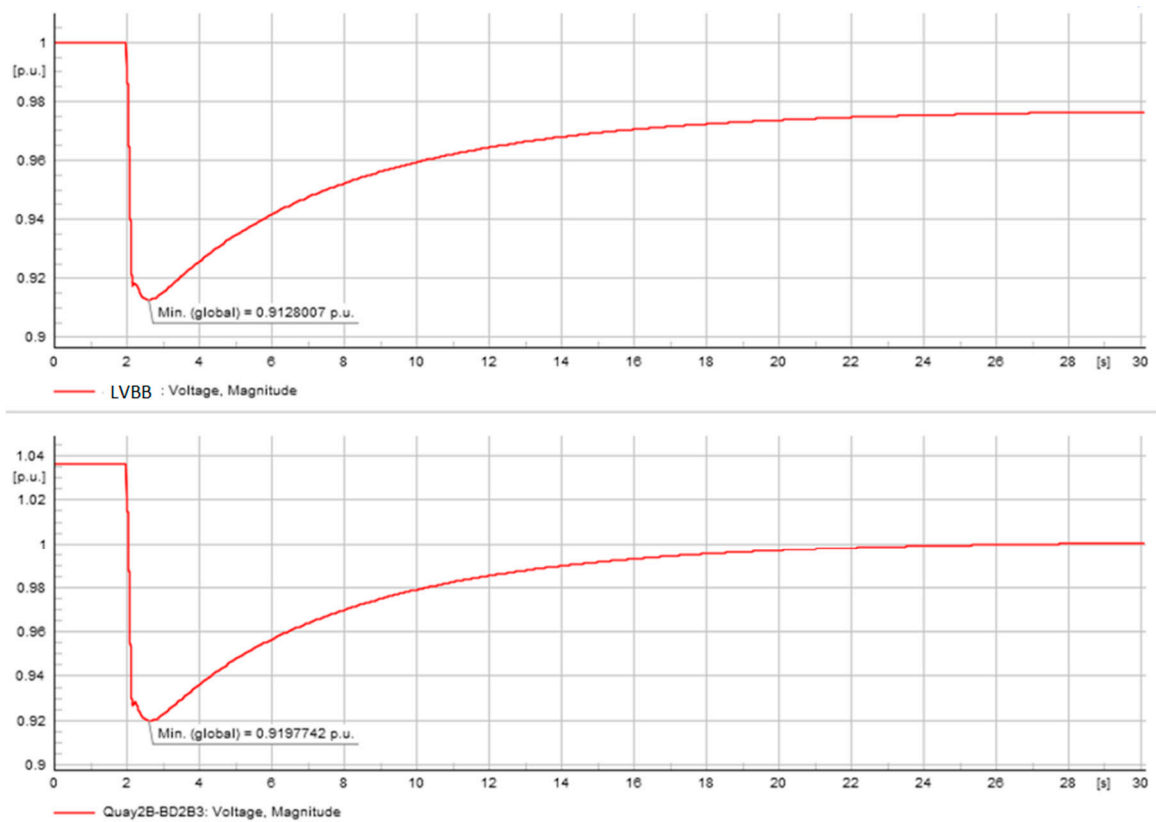
Figure 12. Terminal voltages during load transfer in 11 kV cruise operation mode.

After connection of the load voltage at the ship connection terminals, it drops to approximately 0.917 p.u. (see Figure 13). When a transient process is finished, the voltage level during a new operation mode is established at a level equal to 1 p.u. at ship connection terminals. There is no exceeding of voltage limits observed.
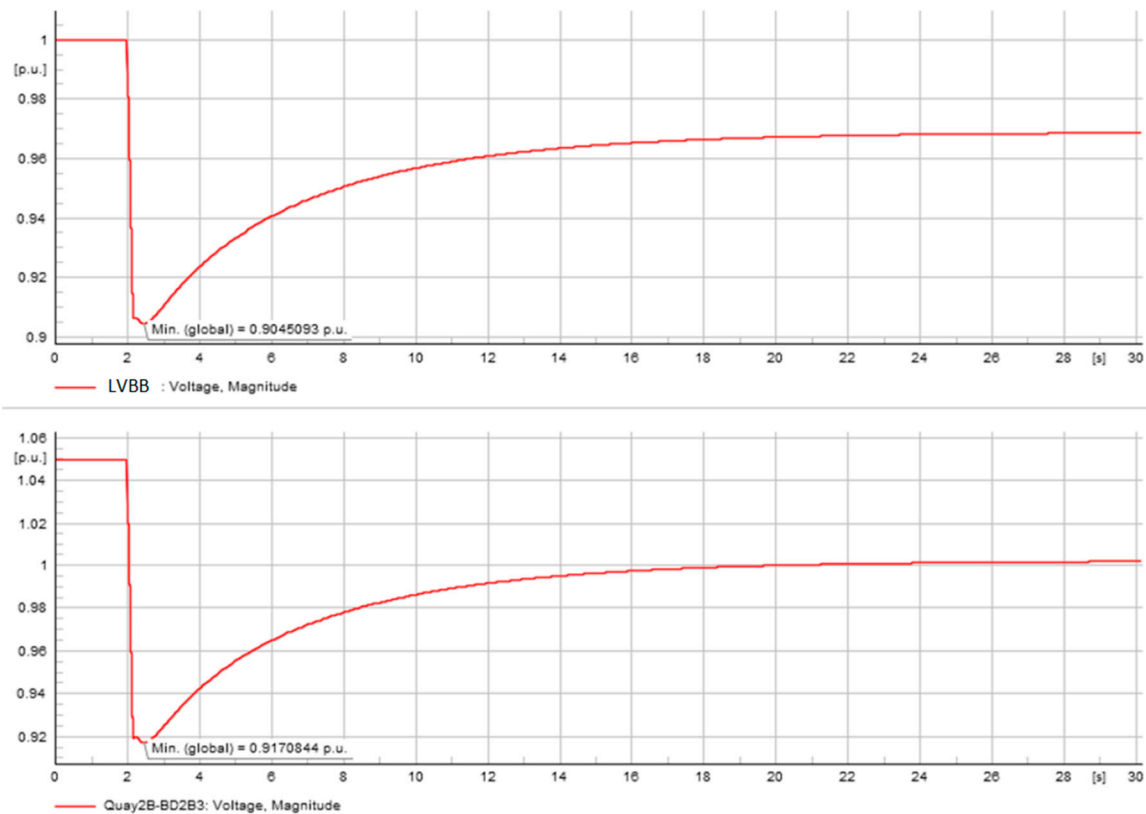
Figure 13. Terminal voltages during load transfer in 6.6 kV cruise operation mode.

c.   *Disconnection of the load from the frequency converter*

In this chapter, simulation results of voltage deviations for load disconnection events are provided.

Initially, when the onboard CB is closed, the load of the vessel is fully powered by the frequency converter. The vessel generator is considered out of service.

After a period of 2 s, the load is stepped down and the onboard CB is opening. When the load is disconnected from the converter, the voltage suddenly increases, and the droop control starts acting until the time when a new steady state is reached. According to simulation results, the new steady state is reached in approximately 70–80 ms.

i.   Disconnection of the load from the frequency converter in 11 kV ferry operation mode

In this chapter, voltage deviations at ferry berths are investigated. According to the simulation results provided, voltage surges appear after the electrical load reaches a value of 1.105 p.u. (see Figure 14). There is no exceeding of voltage limits observed.

ii.   Disconnection of the load from the frequency converter in 11 kV cruise operation mode

In this chapter, voltage deviations at cruise berths are investigated. According to the simulation results provided, the voltage surges that appear after the electrical load reach the value of 1.086 p.u. (see Figure 15). There is no exceeding of voltage limits observed.

iii.   Disconnection of the load from the frequency converter in 6.6 kV cruise operation mode

In this chapter, voltage deviations at cruise berths are investigated. According to the simulation results provided, the voltage surges that appear after the electrical load reach the value of 1.010 p.u. (see Figure 16). There is no exceeding of voltage limits observed.
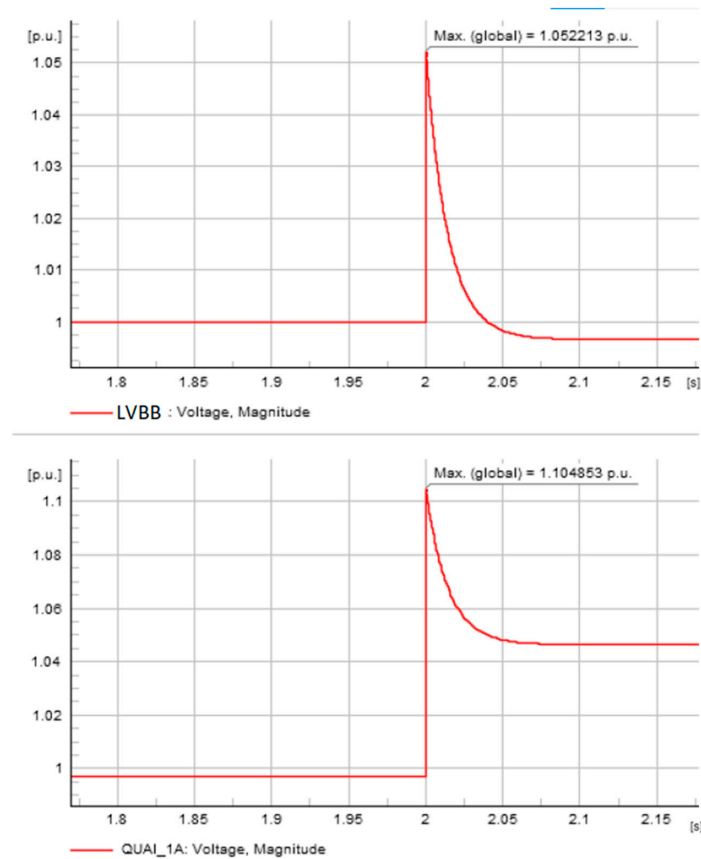
Figure 14. Terminal voltages during disconnection of the load in 11 kV ferry operation mode.
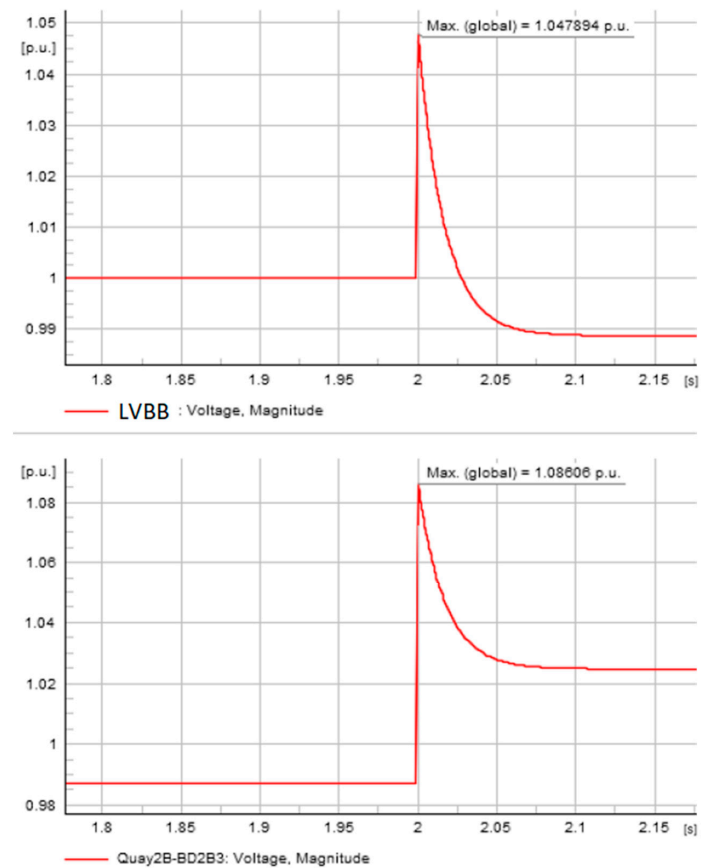
Figure 15. Terminal voltages during disconnection of the load in 11 kV cruise operation mode.
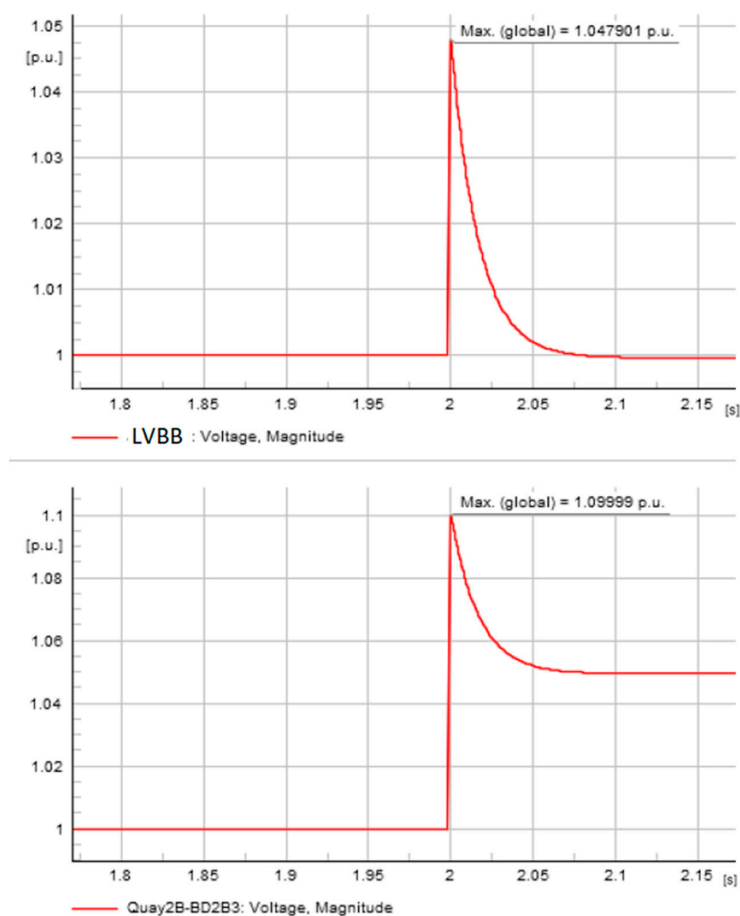
Figure 16. Terminal voltages during disconnection of the load in 6.6 kV cruise operation mode.

6. Conclusions

The article proposed a new option for frequency converters for complex systems with larger outputs, such as shore connection of a large ship. It is the ABB ACS880 SFC, a frequency converter developed for driving motors with modified firmware for use as a static frequency converter. Compared to state-of-the-art solutions, proposed frequency converters can have increased power output per unit, an accessible DC link, and better ability to maintain the voltage in allowed limits. Furthermore, it was voltage deviations during shore connection that were investigated. The port network was created in DIgSILENT PowerFactory. The simulation of droop control of the ABB ACS880 SFC frequency converter was performed during three transient events: connection of the load to the frequency converters; connection of the onboard generators with load transfer; and disconnection of the load from the frequency converters. The simulation results confirmed that the combination of a proper tap-changer position and a droop-controlled frequency converter can be a suitable solution for shore connection in ports in areas with a 50 Hz network frequency. The maximum voltage drop was observed during connection of onboard generators with load transfer in 11 kV ferry operation mode and its value was 0.915 p.u. The maximum voltage surge was observed during load disconnection in 11 kV ferry operation mode and its value was 1.104 p.u. These values are still within limits because, according to marine classification rules, the transient voltage variation can be up to ±20%. Due to proper tap-changer position, steady-state voltage values were also within limits according to international standards (from 0.97 to 1.06 p.u.).

Author Contributions: Software, S.L.; investigation, S.L.; writing—original draft preparation, M.V.; writing—review and editing, R.G. and B.S. All authors have read and agreed to the published version of the manuscript.

Data Availability Statement: Not applicable.

Conflicts of Interest: The authors declare no conflict of interest.

Appendix A
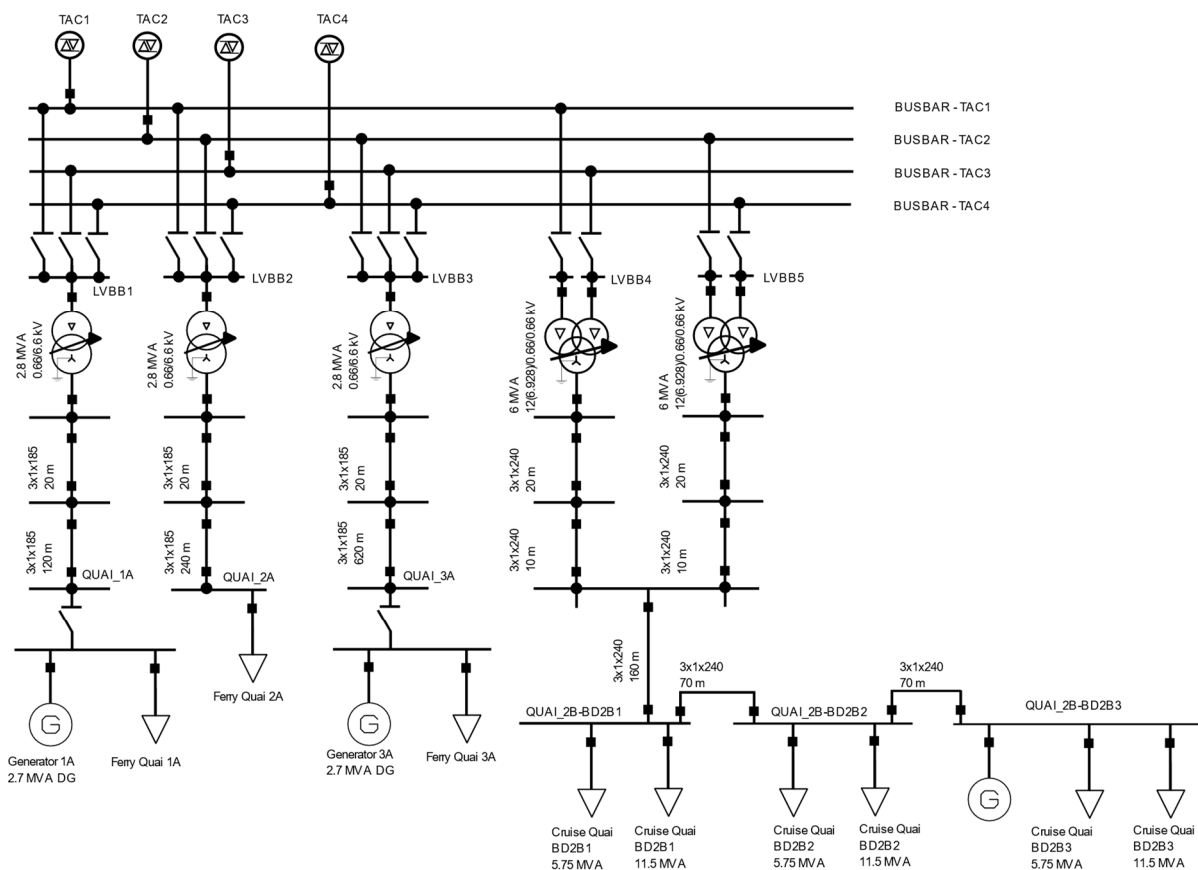
Figure A1. Topology drawing.

References

1. Zanne, M.; Twrdy, E. Air pollution from maritime transport—The problem of today, the challenge of tomorrow. *Pomor. Sci. J. Marit. Res.* **2011**, *24*, 95–102.
2. Innes, A.; Monios, J. Identifying the unique challenges of installing cold ironing at small and medium ports—The case of aberdeen. *Transp. Res. Part D Transp. Environ.* **2018**, *62*, 298–313.
3. Zis, T.P.V. Green Ports. *Sustain. Shipp.* **2019**, 407–432.
4. Stolz, B.; Held, M.; Georges, G.; Boulouchos, K. The CO_2 reduction potential of shore-side electricity in Europe. *Appl. Energy* **2021**, *285*, 116425.
5. Alver, F.; Saraç, B.A.; Alver Şahin, Ü. Estimating of shipping emissions in the Samsun Port from 2010 to 2015. *Atmos. Pollut. Res.* **2018**, *9*, 822–828.
6. Hare, B.; Atkinson-Hope, G. *Harmonic Measurements on Ships and Cold-Ironing*; Under Grad Research; Cape Peninsula University of Technology: Cape Town, South Africa, 2010.
7. Annex, M.E.P.C. *Resolution MEPC.304 (72): Initial IMO Strategy on Reduction of GHG Emissions from Ships*; Maritime Org. (IMO): London, UK, 2018.
8. European Commission, Directorate-General for Communication. *The European Green Deal*; Publications Office: Brussels, Belgium, 2019.
9. Zis, T.P.V. Prospects of cold ironing as an emissions reduction option. *Transp. Res. Part A Policy Pract.* **2019**, *119*, 82–95.
10. Prousalidis, J.; Lyridis, D.; Dallas, S.; Soghomonian, Z.; Georgiou, V.; Spathis, D.; Kourmpelis, T.; Mitrou, P. Ship to shore electric interconnection: From adolescence to maturity. In Proceedings of the 2017 IEEE Electric Ship Technologies Symposium (ESTS), Arlington, VA, USA, 15–17 August 2017; Volume 119, pp. 200–206.

11. International Maritime Organization (IMO). Available online: http://glomeep.imo.org/technology/shore-power (accessed on 10 October 2022).
12. D'Agostino, F.; Schiapparelli, G.P.; Dallas, S.; Spathis, D.; Georgiou, V.; Prousalidis, J. On Estimating the Port Power Demands for Cold Ironing Applications. In Proceedings of the 2021 IEEE Electric Ship Technologies Symposium (ESTS), Arlington, VA, USA, 4–6 August 2021; pp. 1–5.
13. Tarnapowicz, D.; German-Galkin, S. International Standardization in the Design of "Shore to Ship"—Power Supply Systems of Ships in Port. *Manag. Syst. Prod. Eng.* **2018**, *26*, 9–13. [CrossRef]
14. D'Agostino, F.; Grillo, S.; Infantino, R.; Pons, E. High-Voltage Shore Connection Systems: Grounding Resistance Selection and Short-Circuit Currents Evaluation. *IEEE Trans. Transp. Electrif.* **2022**, *8*, 2608–2617.
15. Prenc, R.; Vučetić, D.; Cuculić, A.; Pons, E. High Voltage Shore Connection in Croatia: Network configurations and formation of the connection point to the Utility power grid. *Electr. Power Syst. Res.* **2018**, *157*, 106–117. [CrossRef]
16. Kirkby, L.J.N. South-Western Sub-Centre: Chairman's address. *Electrical shore supplies to ships in HM Dockyards. Proc. Inst. Electr. Eng.* **1964**, *111*, 373.
17. Yang, X.; Bai, G.; Schmidhalter, R. Shore to ship converter system for energy saving and emission reduction. In Proceedings of the 8th International Conference on Power Electronics-ECCE Asia, Jeju, Republic of Korea, 30 May–3 June 2011; pp. 2081–2086.
18. Kumar, J.; Kumpulainen, L.; Kauhaniemi, K. Technical design aspects of harbour area grid for shore to ship power: State of the art and future solutions. *Int. J. Electr. Power Energy Syst.* **2019**, *104*, 840–852.
19. Cuculić, A.; Vučetić, D.; Tomas, V. High voltage shore connection. In Proceedings of the 53rd International Symposium ELMAR-2011, Zadar, Croatia, 14–16 September 2011; pp. 257–259.
20. ABB. PCS100 SFC Static Frequency Converter. Technical Catalogue. 2021. Available online: https://search.abb.com/library/Download.aspx?DocumentID=2UCD030000E009&LanguageCode=en&DocumentPartId=&Action=Launch (accessed on 10 January 2023).
21. ABB; Bernacchi, R. Shore-to-Ship Power Solutions: Static Frequency Conversion Platforms. 2019. Available online: https://search.abb.com/library/Download.aspx?DocumentID=%20%20%209AKK107045A2343%20&LanguageCode=en&DocumentPartId=PDF&Action=Launch (accessed on 10 January 2023).
22. ABB. Enabling the Shore-to-Ship Power Connection: Static Frequency Converters. 2011. Available online: https://library.e.abb.com/public/b948668fe0c03b60c1257daa0056b4e8/ABB%20converters_S2S_product%20guide%20revG.pdf (accessed on 10 January 2023).
23. ABB. ACS880 Multidrives, Optimal Grid Control (Option +N8053). 2022. Available online: https://search.abb.com/library/Download.aspx?DocumentID=3AXD50000220717&LanguageCode=en&DocumentPartId=1&Action=Launch (accessed on 10 January 2023).
24. Kokkonda, R.K.; Kumar, A.; Anurag, A.; Kolli, N.; Parashar, S.; Bhattacharya, S. Medium Voltage Shore-to-Ship Connection System Enabled by Series Connected 3.3 kV SiC MOSFETs. In Proceedings of the 2021 IEEE Applied Power Electronics Conference and Exposition (APEC), Virtual, 14–17 June 2021; pp. 1380–1387.
25. ABB. ACS880-107 Inverter Units. Hardware Manual. 2020. Available online: https://library.abb.com/d/3AUA0000102519 (accessed on 20 May 2023).
26. *P80005-1 ED2*; Utility Connections in Port-Part I: High Voltage Shore Connection (HVSC) Systems—General Requirements. IEC: Geneva, Switzerland, 2018.
27. Chou, M.-H.; Su, C.-L.; Lee, Y.-C.; Chin, H.-M.; Parise, G.; Chavdarian, P. Voltage-Drop Calculations and Power Cable Designs for Harbor Electrical Distribution Systems with High Voltage Shore Connection. *IEEE Trans. Ind. Appl.* **2017**, *53*, 1807–1814. [CrossRef]
28. Zhu, X.; Wang, K.; Yang, J.; Huang, L.; Shen, B.; Sun, M. Research on the control strategy of grid connection between shore power supply and ship power grid. *Energy Rep.* **2022**, *8*, 638–647.
29. Jansen, R.; Timmons, S. *6.6 kV Shore Connection System Description*; ABB Process Automation Marine & Ports: Houston, TX, USA, 2021.
30. Gonen, T. *Electric Power Distribution Engineering*, 3rd ed.; Taylor & Francis: New York, NY, USA, 2014.